PAPER

Magnetically coupled Fano resonance of dielectric pentamer oligomer

IOP Publishing Journal of Physics D: Applied Physics
J. Phys. D: Appl. Phys. **50** (2017) 275002 (6pp) https://doi.org/10.1088/1361-6463/aa7355

Magnetically coupled Fano resonance of dielectric pentamer oligomer

Fuli Zhang[1], Chang Li[1,2], Xuan He[1], Lei Chen[1], Yuancheng Fan[1], Qian Zhao[3], Weihong Zhang[4] and Ji Zhou[5]

[1] Key Laboratory of Space Applied Physics and Chemistry, Ministry of Education and Department of Applied Physics, School of Science, Northwestern Polytechnical University, Xi'an 710072, People's Republic of China
[2] Center for Quantum Information, Institute for Interdisciplinary Information Sciences, Tsinghua University, Beijing 100084, People's Republic of China
[3] State Key Lab of Tribology, Department of Mechanical Engineering, Tsinghua University, Beijing 100084, People's Republic of China
[4] School of Mechanical Engineering, Northwestern Polytechnical University, Xi'an 710072, People's Republic of China
[5] State Key Lab of New Ceramics and Fine Processing, Department of Materials Science and Engineering, Tsinghua University, Beijing 100084, People's Republic of China

E-mail: fuli.zhang@nwpu.edu.cn

Received 8 February 2017, revised 13 April 2017
Accepted for publication 16 May 2017
Published 15 June 2017

Abstract

We present magnetically induced Fano resonance inside a dielectric metamaterial pentamer composed of ceramic bricks. Unlike previous reports where different sizes of dielectric resonators were essential to produce Fano resonance, under external magnetic field excitation, central and outer dielectric bricks with identical sizes exhibit in-phase and out-of-phase magnetic Mie oscillations. An asymmetric line shape of Fano resonance along with enhanced group delay is observed due to the interference between the magnetic resonance of the central brick and the symmetric magnetic resonance of outer bricks. Besides, Fano resonance blueshifts with the increasing resonance of the smaller central brick. The thermal-dependent permittivity of ceramics allows Fano resonance to be reversibly tuned by 300 MHz when temperature varies by 60 °C.

Keywords: metamaterial, temperature, Mie scattering

(Some figures may appear in colour only in the online journal)

Introduction

Recently, Fano resonance has attracted a great deal of attention [1–36] due to its asymmetric line shape and related ability for high-quality factors. These unique properties are of particular interest in potential applications, including nonlinear effects, sensing and filters [26, 27, 29, 31–36]. It originally arises from interference between direct- and indirect-resonance-assisted pathways inside atomic and other quantum wells in semiconductors. Recently, Fano resonance has been demonstrated via the near field coupling effect of subwavelength metamaterials. To resemble the original physics, i.e. interference of a narrow discrete resonance with a broad spectral line in quantum systems, superradiant bright mode and subradiant dark mode with different scattering pathways were proposed. What is more, the Fano resonance is also original from the interference of non-orthogonal eigenmodes in the oligomer structure [9]. The main obstacle to generate Fano resonance is how to delicately engineer a subradiant mode which can strongly couple with the bright mode. To satisfy such a requirement, geometry asymmetry has been widely used in microstructure design to induce a dark mode.

However, most Fano resonances were observed under incident electric field excitation, whereas those reliant on magnetic field excitation were rarely exploited [4–9]. The main limitations arise from the requirements of proper polarization

and sample preparation, which become more challenging at optical range. One solution is to employ titled incidence with a magnetic field component perpendicular to the microstructure plane. Shafiei *et al* present experimentally magnetic-coupled Fano resonance via four nanorings with small structural asymmetries [4]. Very recently, the collective resonance of dielectric clusters has been engineered to produce Fano resonance [5–13, 35]. Different from the LC resonance mechanism, the local field is mostly concentrated inside dielectric resonators. To produce Fano resonance inside dielectric oligomers, a novel idea of employing dielectric heptamer oligomers with different size particles was first proposed [5]. In such a configuration, central and outer particles oscillate out of phase at a specific frequency between their respective eigenfrequencies, resulting in the strong suppression of radiation.

Unlike previous works in which different dielectric particles are essential to realize out-of-phase resonances, we present a magnetically induced Fano resonance inside a dielectric pentamer composed of identical ceramic bricks. Experimental and numerical results reveal that a sharp Fano resonance characterized by an asymmetric line shape is observed when a dielectric brick is inserted into the center of four densely-stacked dielectric bricks. The central brick oscillates out of phase with respect to the collective resonance of dielectric oligomers, leading to destructive interference. The Fano resonance of dielectric pentamers proposed herein is sensitivity to the interspacing separation between central and outer bricks. At last, the thermal tunable Fano resonance property is experimentally verified.

Experiment

A rectangular ceramic brick with 3.5 mm × 3.5 mm × 1 mm was selected as the building block for metamaterials oligomers. Calcium titanate ($CaTiO_3$) doped by 1 wt%Z_rO_2 ($\varepsilon_r = 123$, $\tan\delta = 0.001$) is employed as the building block for dielectric oligomers due to its high relative permittivity and low dielectric loss [36, 37]. Teflon substrate ($\varepsilon_r = 2.1$, $\tan\delta = 0.001$) was cut into a rectangular brick of 20 × 16 × 1 mm. Using a digital control milling machine, five slots were made on Teflon substrate to hold the dielectric ceramic bricks. The larger length of the outer slot compared to the central one enables the change of interspacing distance between the outer and center ceramic bricks. Finally, dielectric metamaterial oligomers were assembled by inserting dielectric bricks into the Teflon template.

Figure 1 shows the dielectric pentamer metamaterial which comprises four outer ceramic bricks and one central brick. These five dielectric bricks share the same size. The four outer ceramic bricks are placed on two mutually orthogonal planes and separated with the same distance to the central brick, forming a tetramer-like oligomer. A Teflon substrate with pentamer-type slots is prepared as the template to hold dielectric bricks. The whole pentamer metamaterial is excited by an incident wave polarized with an electric field along the x axis and a magnetic field along the y axis, respectively. Obviously, the central brick has its largest surface perpendicular to the incident magnetic field, whereas the outer brick has a 45° inclination. The scattering parameters were measured in a standard X band rectangular waveguide and recorded by using a vector network analyzer (VNA) AV3629D.

Results and discussion

Figure 2 gives the transmission spectra for the central brick alone, with the tetramer and pentamer at room temperature of 30.0 °C. As observed in figure 2, the central brick exhibits a well-pronounced transmission dip at around 8.935 GHz, which is presumably a magnetic Mie excitation due to the ground mode resonance observed experimentally. Tetramer metamaterial with an interspacing separation of $d = 3.5$ mm produces two transmission dips at 8.75 GHz and 9.06 GHz, respectively. As an identical dielectric brick is inserted into the central position of the tetramer, although two transmission dips are still preserved, a sharp transmission Fano peak characterized by an asymmetric spectral line shape is observed at 8.69 GHz, which is completely different from that of a dielectric tetramer. Using the Fano equation [38], we can obtain a quality factor as high as 200, which is compared to that obtained inside a metallic microstructure [24]. It is worth noting that such high Q can be still preserved inside dielectric oligomers at optical range [10, 35].

To check the validity of transmission spectra evolution from one brick, tetramer to pentamer, full wave simulations were carried out to calculate the scattering parameters. From the comparison between figures 2(a) and (b), an excellent agreement between experiment and simulation can be observed. Both confirm the asymmetric Fano spectra characteristic of the pentamer oligomer. The slight discrepancies of an experimental transmission dip in strength around the Fano peak and an extra ripple at 8.75 GHz are mainly attributed to a minor inaccurate assembly of the oligomer.

To exploit the underlying mechanism of various resonances, local magnetic fields in the xy plane are monitored for related transmission dips and peaks (see figure 2(b)) and depicted in figure 3. For the dielectric brick alone, a magnetic dipole resulting from circulating displacement currents oscillates along the y axis around its resonance dip, confirming the magnetic resonance characteristic, as mentioned in the previous assumptions. In the tetramer structure, four bricks normally tilted by 45° have the largest surface totally projected onto the incident magnetic field. The front and rear dielectric bricks exhibit magnetic dipole resonance stimulated by the incident magnetic field. Due to the in-phase and out-of-phase oscillations between their magnetic dipoles, the spectra split into two eigenmodes, namely the symmetric and antisymmetric magnetic resonance modes.

As observed in figure 3, the front and rear dielectric resonators exhibit in-phase oscillation, resulting in a strong magnetic moment at spectral position 3. By contrast, the front and rear dielectric resonators exhibit out-of-phase oscillations at spectral position 2. Thus, the induced magnetic moments are directed oppositely to each other, leading to head-to-tail configuration, i.e. toroidal dipole moment [39, 40]. As the incident wave passes through the dielectric oligomer along the z

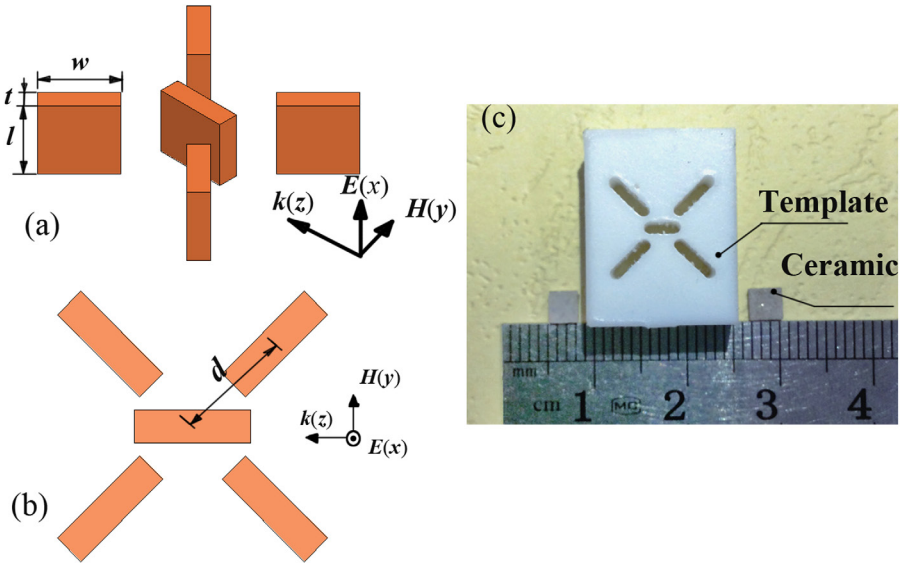

Figure 1. (a) Close-up and (b) top view of pentamer oligomer metamaterial. (c) Photograph of dielectric ceramic brick and Teflon template. The outer slots have larger length than that of the central one, such that the distance between central and outer ceramic resonators can be modified. The geometry dimensions of dielectric bricks are set as $w = l = 3.5$ mm, $t = 1.0$ mm.

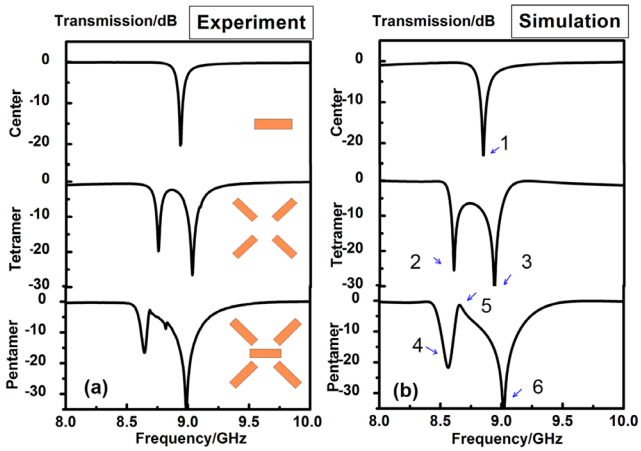

Figure 2. Transmission spectra of central brick, tetramer and pentamer metamaterials. (a) Experiment (left column) (b) simulation (right column). Insets present single brick (top), tetramer (middle) and pentamer (bottom) dielectric oligomer configuration.

direction, the rear resonators resonate at a lower magnitude than those of the front bricks. In the pentamer structure, when an extra identical dielectric brick is inserted into the center, the original resonances of the tetramer are disturbed. At lower resonance dip 4, magnetic resonance of the central brick is still predominant since external magnetic field is directly perpendicular to its largest plane, while the other four bricks are excited by magnetic field vertical component to their surfaces. Due to the presence of the central brick, the interaction between the front and rear outer bricks is disturbed and becomes weaker.

At spectral position 6, the central brick shows an in-phase oscillation with the outer bricks, resulting in a collective strong net dipole moment. From the comparison with local field intensities of position 3, despite a decrease in resonance strength inside the front and rear bricks of the pentamer, the presence of the central brick compensates this reduction and contributes to a deepened transmission dip (see figure 2). By contrast, the local magnetic field of the central brick is dramatically increased and opposite to that of the outer bricks at spectral position 5. The out-of-phase oscillations between central and outer bricks result in a vanishing net dipole moment. As a consequence, the dielectric pentamer weakly couples to the incident wave and resonates as the subradiant mode. The destructive interference between superradiant and subradiant modes accounts for the emergence of asymmetric Fano resonance. The enhancement of local field intensity corresponds to the high quality factor of Fano resonance.

To further clarify the underlying physics of Fano resonance in pentamer oligomers, the influences of the central brick size are studied and given in figure 4. The central brick width, w, as depicted in figure 1, is gradually decreased from 3.5 mm down to 2.9 mm, while the geometry dimensions of the outer bricks are kept the same as $3.5 \times 3.5 \times 1.0$ mm. Unlike the pentamer with identical bricks whose Fano peak is below the symmetric mode of the outer bricks, as the central brick width decreases below 3.5 mm, Fano resonance still exists but its location emerges between symmetric collective magnetic resonances of the outer bricks and magnetic resonance of the central brick. The antisymmetric and symmetric resonances of the tetramer remain nearly the same, due to the unchanged size and configuration of the outer bricks. Besides, Fano resonance peaks shift towards higher frequencies when magnetic resonance of central bricks increases. This clearly demonstrates that Fano resonance originates from the interference between outer and central bricks.

In addition, the influences of interspacing separation between dielectric bricks on Fano resonance are investigated and presented in figure 5. As the interspacing separation, d, increases gradually from 3.5 mm to 4.5 mm, The Fano resonance and antisymmetric resonance shift towards higher frequencies, due to the decreasing coupling effect. Moreover, the resonance strength of the antisymmetric mode decays rapidly,

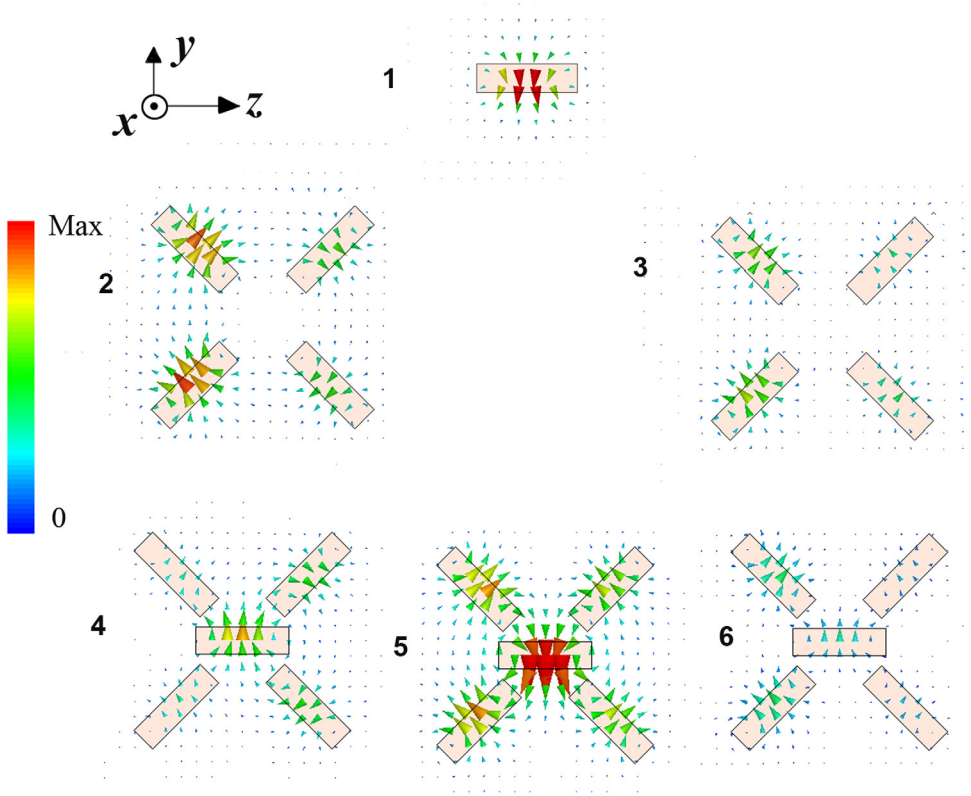

Figure 3. Local magnetic field distributions for the center brick, tetramer, and pentamer oligomer at respective spectral positions, as indicated by arrows in figure 2. All the fields have been normalized to the same scale for comparison.

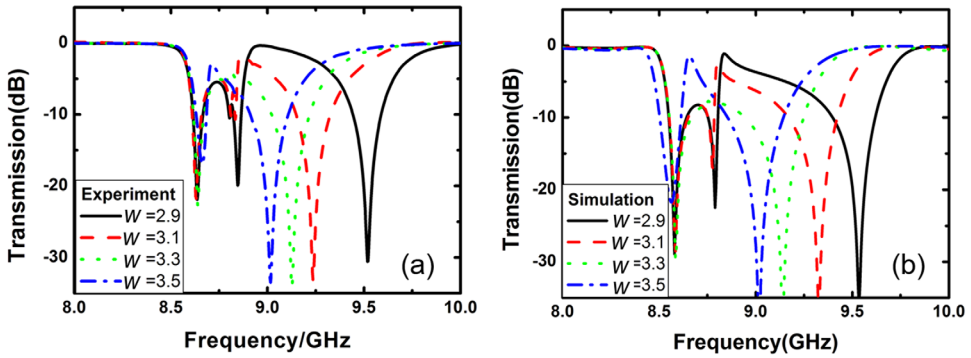

Figure 4. The influences of central brick width, w, on Fano resonance (a) experiment (b) simulation. The other side length of central brick, l, and neighboring distance, d, are fixed as 3.5 mm.

so that it almost vanishes into a spectral envelope of collective magnetic resonance. This is because the adjunction of the central brick disturbs the original antisymmetric resonance mode of tetramer, as shown in figure 2. As the outer bricks move away from the central brick, the interaction inside outer bricks decreases and results in a weakened transmission dip, which makes Fano spectral profile not so pronounced. However, Fano resonance is nearly independent from interspacing variation for the pentamer with a smaller central brick. As shown in figures 5(c) and (d), oligomer with central brick width $w = 3.1$ mm exhibits a magnetic resonance around 9.25 GHz, which is higher than symmetric mode of tetramer. In this case, experimental and numerical results demonstrate that Fano resonance is almost stable as the interspacing distance increases from 3.5 mm to 4.5 mm. Besides, the unchanged spectral profile of resonance modes of outer bricks indicates central brick influence is probably negligible when its magnetic resonance is much higher than the symmetric resonance of outer bricks.

At last, dynamically tune magnetic-coupled Fano resonance is verified experimentally. By taking benefit of the temperature dependent permittivity of ceramic, we realize a thermally controllable Fano resonance as shown in figure 6. When temperature increases from 0 °C to 60 °C, Fano peak experiences a visible blueshift from 8.58 GHz to 8.87 GHz, because of the decreasing relative permittivity of the ceramic [41–45].

The group delay of metamaterial pentamer, $\tau(\omega) = \mathrm{d}\phi(\omega)/\mathrm{d}\omega$, was also measured by VNA and given in figure 7(a). We can observe an enhanced group delay of 11.0 ns around Fano

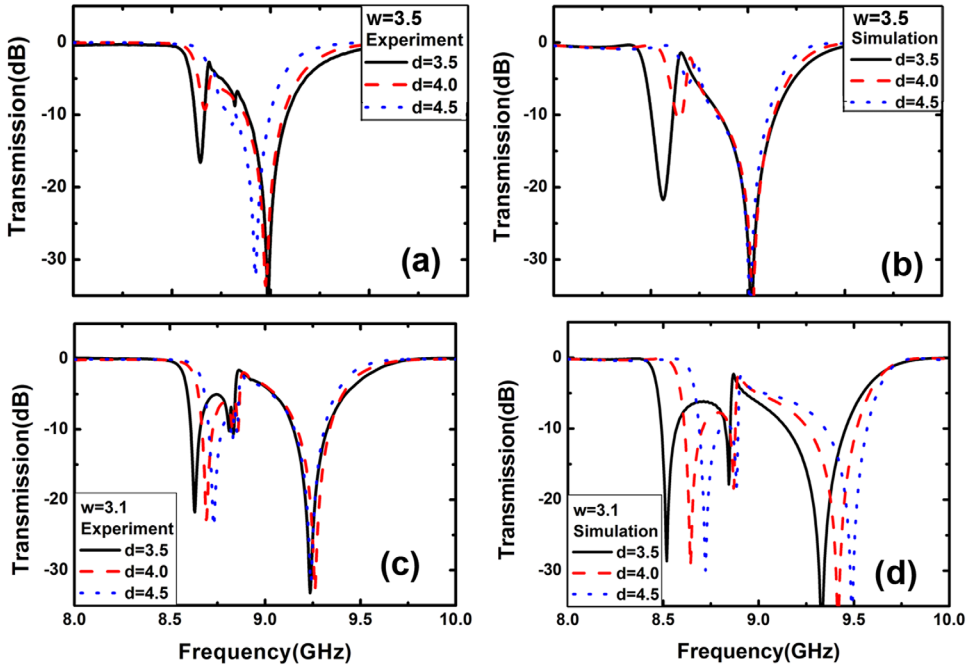

Figure 5. Experimental (a) and (c) and numerical (b) and (d) transmission spectra of pentamer metamaterial versus interspacing separation, *d*, between central and outer bricks.

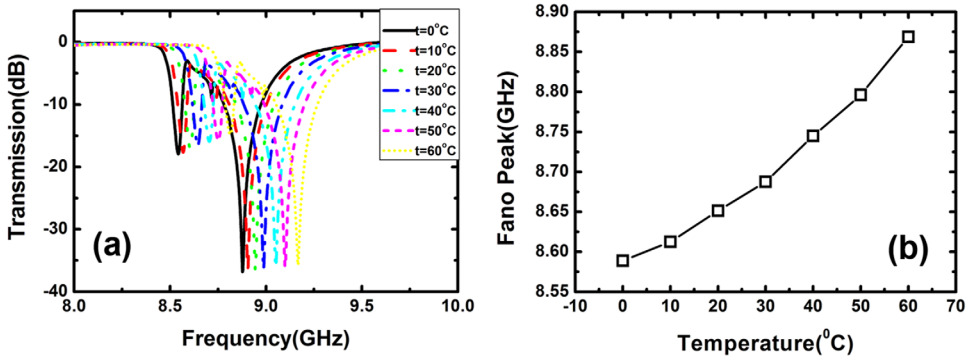

Figure 6. Experimental transmission spectra (a) and Fano resonance peak (b) of pentamer metamaterial under different temperature.

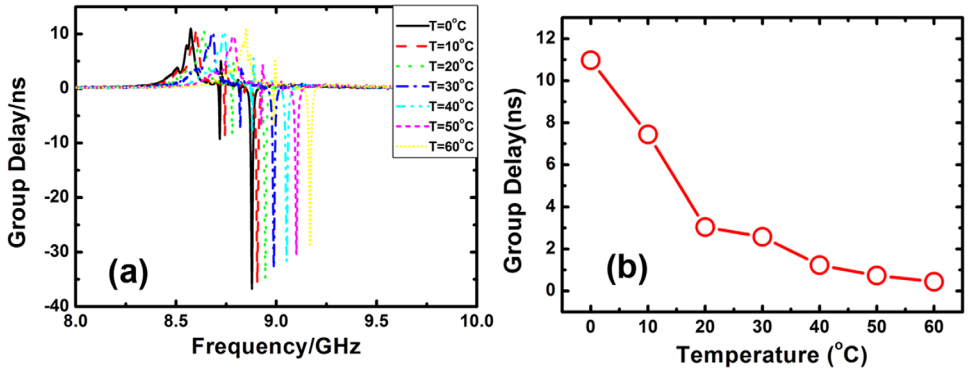

Figure 7. Group delay of pentamer metamaterial under various temperatures. (a) Frequency spectra (b) group delay dependence on temperature variation at 8.58 GHz.

peak, corresponding to the slowdown of electromagnetic wave by a factor of 200 with respect to free-space propagation, given the thickness of pentamer is assumed as 15 mm. Similar to the transmission spectra dependence on temperature, the group delay peak blueshifts accordingly with the increasing temperature. Furthermore, such a temperature dependent property enables the dynamic control of signal transmission delay at a specific frequency of interest. Take the Fano peak at 8.58 GHz for instance; the incident beam passing through dielectric pentamer experiences a group delay change by 11 ns when the temperature changes by 60 °C, as shown in figure 7(b).

Conclusion

In summary, magnetically induced Fano resonance is experimentally verified inside a dielectric brick oligomer. In a pentamer configuration, central and outer bricks exhibit in-phase and out-of-phase oscillations, corresponding to superradiant and subradiant modes, respectively. An asymmetric line shape of Fano resonance, arising from destructive interference between the magnetic resonance of central brick and collective magnetic resonance mode of oligomer, is observed. Therefore, such Fano resonance strongly relies on the interaction between the central brick and outer bricks. Besides, the Fano peak is reversibly tuned around 300 MHz when environmental temperature varies by 60 °C. Such a dynamic frequency shift enables a group delay to be modified by 11 ns at a specific frequency of interest. Compared to metallic microstructure, low loss advantage of dielectric metamaterial is more remarkable at higher frequencies; the dielectric oligomer proposed herein provides one extra means to realize high-Q Fano resonance at optical regime.

Acknowledgment

This work is funded from National Natural Science Foundation of China (NSFC) (Grant Nos. 11372248, 61505164, 61275176, 51532004, and 51221001), Shaanxi Project for Young New Star in Science and Technology (Grant No. 2015KJXX-11), and Program for New Century Excellent Talents in University.

References

[1] Luk'yanchuk B, Zheludev N I, Maier S A, Halas N J, Nordlander P, Giessen H and Chong C T 2010 *Nat. Mater.* **9** 707
[2] Miroshnichenko A E, Flach S and Kivshar Y S 2010 *Rev. Mod. Phys.* **82** 2257
[3] Fan P Y, Yu Z F, Fan S H and Brongersma M L 2014 *Nat. Mater.* **13** 471
[4] Shafiei F, Monticone F, Le K Q, Liu X X, Hartsfield T, Alu A and Li X Q 2013 *Nat. Nanotechnol.* **8** 218
[5] Miroshnichenko A E and Kivshar Y S 2012 *Nano Lett.* **12** 6459
[6] Filonov D S, Slobozhanyuk A P, Krasnok A E, Belov P A, Nenasheva E A, Hopkins B, Miroshnichenko A E and Kivshar Y S 2014 *Appl. Phys. Lett.* **104** 021104
[7] Chong K E, Hopkins B, Staude I, Miroshnichenko A E, Dominguez J, Decker M, Neshev D N, Brener I and Kivshar Y S 2014 *Small* **10** 1985
[8] Hopkins B, Poddubny A N, Miroshnichenko A E and Kivshar Y S 2013 *Phys. Rev.* A **88** 053819
[9] Hopkins B, Filonov D S, Miroshnichenko A E, Monticone F, Alu A and Kivshar Y S 2015 *ACS Photonics* **2** 724
[10] Yang Y M, Kravchenko I I, Briggs D P and Valentine J 2014 *Nat. Commun.* **5** 5753
[11] Yan J H, Liu P, Lin Z Y, Wang H, Chen H J, Wang C X and Yang G W 2015 *Nat. Commun.* **6** 7042
[12] Zhang F L, Huang X C, Zhao Q, Chen L, Wang Y, Li Q, He X, Li C and Chen K 2014 *Appl. Phys. Lett.* **105** 172901
[13] Zhang J F, Liu W, Zhu Z H, Yuan X D and Qin S Q 2014 *Opt. Express* **22** 30889
[14] Cui Y H, Zhou J H, Tamma V A and Park W 2012 *ACS Nano* **6** 2385
[15] Alonso-Gonzalez P *et al* 2011 *Nano Lett.* **11** 3922
[16] Fan J A, Bao K, Wu C H, Bao J M, Bardhan R, Halas N J, Manoharan V N, Shvets G, Nordlander P and Capasso F 2010 *Nano Lett.* **10** 4680
[17] Fan J A, Wu C H, Bao K, Bao J M, Bardhan R, Halas N J, Manoharan V N, Nordlander P, Shvets G and Capasso F 2010 *Science* **328** 1135
[18] Sheikholeslami S N, Garcia-Etxarri A and Dionne J A 2011 *Nano Lett.* **11** 3927
[19] Rahmani M, Lukiyanchuk B, Nguyen T T V, Tahmasebi T, Lin Y, Liew T Y F and Hong M H 2011 *Opt. Mater. Express* **1** 1409
[20] Artar A, Yanik A A and Altug H 2011 *Nano Lett.* **11** 3694
[21] Moritake Y, Kanamori Y and Hane K 2014 *Opt. Lett.* **39** 4057
[22] Cao W, Singh R, Al-Naib I A, He M X, Taylor A J and Zhang W L 2012 *Opt. Lett.* **37** 3366
[23] Papasimakis N and Zheludev N I 2009 *Opt. Photonics News* **20** 22
[24] Fedotov V A, Rose M, Prosvirnin S L, Papasimakis N and Zheludev N I 2007 *Phys. Rev. Lett.* **99** 147401
[25] Fedotov V A, Tsiatmas A, Shi J H, Buckingham R, de Groot P, Chen Y, Wang S and Zheludev N I 2010 *Opt. Express* **18** 9015
[26] Chang W S, Lassiter J B, Swanglap P, Sobhani H, Khatua S, Nordlander P, Halas N J and Link S 2012 *Nano Lett.* **12** 4977
[27] Chen C Y, Un I W, Tai N H and Yen T J 2009 *Opt. Express* **17** 15372
[28] Hentschel M, Saliba M, Vogelgesang R, Giessen H, Alivisatos A P and Liu N 2010 *Nano Lett.* **10** 2721
[29] Lahiri B, Khokhar A Z, De La Rue R M, McMeekin S G and Johnson N P 2009 *Opt. Express* **17** 1107
[30] Liu N, Langguth L, Weiss T, Kastel J, Fleischhauer M, Pfau T and Giessen H 2009 *Nat. Mater.* **8** 758
[31] Wu C H, Khanikaev A B, Adato R, Arju N, Yanik A A, Altug H and Shvets G 2012 *Nat. Mater.* **11** 69
[32] Cao T and Zhang L 2013 *Opt. Express* **21** 19228
[33] Cao T, Zhang L, Xiao Z P and Huang H 2013 *J. Phys. D: Appl. Phys.* **46** 19228
[34] Samson Z L, MacDonald K F, De Angelis F, Gholipour B, Knight K, Huang C C, Di Fabrizio E, Hewak D W and Zheludev N I 2010 *Appl. Phys. Lett.* **96** 143105
[35] Wu C, Arju N, Kelp G, Fan J A, Dominguez J, Gonzales E, Tutuc E, Brener I and Shvets G 2014 *Nat. Commun.* **5** 3892
[36] Zhang F L, Zhao Q, Lan C W, He X, Zhang W H, Zhou J and Qiu K P 2014 *Appl. Phys. Lett.* **104** 131907
[37] Wu H Y, Zhou J, Lan C W, Guo Y S and Bi K 2014 *Sci. Rep.* **4** 5499
[38] Srivastava Y K, Manjappa M, Cong L Q, Cao W, Al-Naib I, Zhang W L and Singh R 2016 *Adv. Opt. Mater.* **4** 457
[39] Fan Y C, Wei Z Y, Li H Q, Chen H and Soukoulis C M 2013 *Phys. Rev.* B **87** 115417
[40] Kaelberer T, Fedotov V A, Papasimakis N, Tsai D P and Zheludev N I 2010 *Science* **330** 1510
[41] Luo T H, Li B, Zhao Q and Zhou J 2015 *Int. J. Antennas Propag.* **2015** 291234
[42] Zhang F L, Chen L, Wang Y, Zhao Q, He X and Chen K 2014 *Opt. Express* **22** 24908
[43] Zhao Q, Du B, Kang L, Zhao H J, Xie Q, Li B, Zhang X, Zhou J, Li L T and Meng Y G 2008 *Appl. Phys. Lett.* **92** 051106
[44] Zhao Q *et al* 2015 *Adv. Mater.* **27** 6187
[45] Zhao Q, Zhou J, Zhang F L and Lippens D 2009 *Mater. Today* **12** 60